Loading an optical dipole trap

S. J. M. Kuppens, K. L. Corwin, K. W. Miller, T. E. Chupp,* and C. E. Wieman

JILA, University of Colorado and National Institute for Standards and Technology, Boulder, Colorado 80309-0440
(Received 18 October 1999; published 13 June 2000)

We present a detailed experimental study of the physics involved in transferring atoms from a magneto-optical trap (MOT) to an optical dipole trap. The loading is a dynamical process determined by a loading rate and a density dependent loss rate. The loading rate depends on cooling and the flux of atoms into the trapping volume, and the loss rate is due to excited state collisions induced by the MOT light fields. From this study we found ways to optimize the loading of the optical dipole trap. Key ingredients for maximum loading are found to be a reduction of the hyperfine repump intensity, increased detuning of the MOT light, and a displacement of the optical dipole trap center with respect to the MOT. A factor of 2 increase in the number of loaded atoms is demonstrated by using a hyperfine repump beam with a shadow in it. In this way we load 8×10^6 ^{85}Rb atoms into a 1 mK deep optical dipole trap with a waist of 58 μm, which is 40% of the atoms initially trapped in the MOT.

PACS number(s): 32.80.Pj

I. INTRODUCTION

In the last decade, many different schemes for preparing and trapping ultracold and dense samples of atoms have been demonstrated. Of these, the optical dipole trap [1] requires no magnetic fields and relatively few optical excitations to provide a conservative and tightly confining trapping potential. These characteristics make it an appealing option for various metrology applications such as parity nonconservation and β-decay asymmetry measurements. It may also be an option for reaching Bose-Einstein condensation in a purely optical trap. For these applications, large samples of atoms must be transferred into the dipole trap. This is almost always done from a magneto-optical trap (MOT) [2]. However, the processes determining the transfer between the MOT and the optical dipole trap are poorly understood. Here we give a detailed description and explanation of the loading process and suggest ways in which to improve the loading.

The simplest optical dipole trap consists of a focused single Gaussian laser beam. Typically, the light is detuned below the atomic resonance, from a few tenths of a nanometer to several tens of nanometers. The latter are called far-off-resonance traps (FORTs) [3]. We will use the abbreviation FORT in discussing optical dipole traps. Conceptually, a FORT works as follows: The ac Stark shift induced by the trapping light lowers the ground state energy of the atoms proportionally to the local intensity. The spatial dependence of the atomic potential energy is therefore equivalent to a spatial dependence of the light intensity. The atom has the lowest energy in the focus of the trapping beam and can therefore be trapped there. For very large detuning, typically several nanometers, the photon scattering rate becomes so low that the potential is truly conservative.

The first FORTs were running-wave Gaussian laser beams focused to a waist of about 10 μm [1,3]. By alternating the FORT with an optical molasses that cooled atoms

into the trap [1,3], about 500 to 1300 atoms were loaded. In later work [4–6], the FORT was loaded by overlapping it with a MOT continuously, which improved the number of atoms that was transferred to 10^6.

A key step in the loading of a FORT from a MOT is a strong reduction of the hyperfine repump power in the last 10–30 ms of the overlap between the traps. It has been conjectured [4] that this reduction helps because it reduces three density limiting processes, namely, radiative repulsion forces, photoassociative collisions, and ground state hyperfine changing collisions. However, to our knowledge, there has not yet been an extensive study of the loading process. Therefore, in this paper we present a detailed and comprehensive investigation of the many mechanisms that govern the loading process.

We find that loading a FORT from a MOT is an interesting dynamical process rich in physics. As illustrated in Fig. 1, the number of atoms in the FORT first increases rapidly and nearly linearly in time until loss mechanisms set a limit to the maximum number. The loading rate and loss processes both depend in complex ways on the laser fields involved. One factor that determines the loading rate is the flux of atoms into the trapping volume. This flux depends on the MOT density and temperature, i.e., average velocity, of the
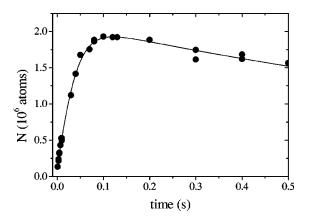

FIG. 1. Number of atoms N in the FORT during loading, for a trap depth of 1 mK and a waist of 26 μm.

62 013406-1

atoms in the MOT. Cooling mechanisms must also be active in the region where the MOT and FORT overlap for the atoms to be trapped in the FORT. Both the flux and the probability for trapping depend on the trap depth and light shifts inherent to the FORT.

Losses from the trap can be caused by heating mechanisms and collisional processes. Contributions to heating arise from spontaneously scattered FORT light photons, background gas collisions [7,8], intensity fluctuations, and the pointing stability of the FORT beam [9]. However, for large numbers of atoms, the losses are dominated by collisional processes [10], including photoassociation, spin exchange/ground state hyperfine changing collisions, and radiative escape. Photoassociative collisions can be induced by the FORT light itself and lead to untrapped molecules. During a ground state hyperfine changing collision the atoms gain as much as the hyperfine energy splitting in kinetic energy (0.14 K for ^{85}Rb), which is enough to eject them out of the FORT. In radiative escape, an atom is optically excited and reemits during a collision, and the attractive dipole-induced interaction between the excited and nonexcited atoms leads to an increase of kinetic energy that is enough to eject an atom from the trap.

The loading and loss rates depend on the shape and depth of the optical potential, as well as the intensity and detuning of the MOT light fields. By studying the loading rate and loss rate separately as a function of these parameters we have obtained a detailed understanding of the FORT loading process. This understanding has allowed us to optimize parameters in order to improve our loading efficiency to high values. Although we studied the loading of ^{85}Rb into a dipole trap with a detuning of a few nanometers, the physical processes and optimization should be generally applicable to other alkali-metal species and FORTs, when the FORT trap depth exceeds the MOT atom temperature. In the opposite regime, O'Hara *et al.* [11] have shown that a static equilibration model applies in CO_2 laser traps.

This paper is organized as follows. In Sec. II, a more detailed expression for the depth and shape of the FORT potential is given. In Sec. III, our experimental setup is discussed, including the loading of the FORT and the diagnostic tools for measuring the number of atoms and size of the trapped sample. In Sec. IV, we present measurements of the loading rate and loss rate as a function of different MOT and FORT parameters. In Sec. V, the temperature of the atoms in the FORT is given. In Sec. VI, the loss rates of the FORT in the absence of MOT light are discussed. In Sec. VII, we present a physical model of the loading process that explains the data presented in Sec. IV. In Sec. VIII, we discuss how our model explains the interdependencies of the MOT and FORT parameters. In Sec. IX, we demonstrate how, based on our understanding of the FORT loading process, the number of trapped atoms can be improved using a shadowed repump beam. Finally, Sec. X contains summarizing remarks and discusses the general applicability of our results to other traps.

II. FORT POTENTIAL

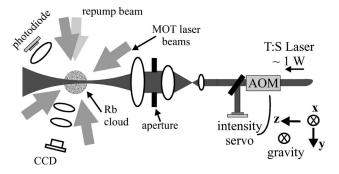The trapping potential is given by the Gaussian shape of the laser beam,

FIG. 2. Experimental setup.

$$U(r,z) = U_0 \frac{\exp[-2r^2/w(z)^2]}{1+(z/z_R)^2}, \qquad (1)$$

with r and z the radial and longitudinal coordinates, $w(z) = w_0\sqrt{1+(z/z_R)^2}$ the beam radius as a function of longitudinal position, and z_R the beam Rayleigh range [12]. For an alkali-metal atom, the depth of the potential U_0 is calculated from [13]

$$U_0 = \frac{\hbar\gamma I_0}{24I_S}\left[\left(\frac{1}{\delta_{1/2}} + \frac{2}{\delta_{3/2}}\right) - g_F m_F\sqrt{1-\epsilon^2}\left(\frac{1}{\delta_{1/2}} - \frac{1}{\delta_{3/2}}\right)\right], \qquad (2)$$

where γ is the natural linewidth, m_F is the Zeeman sublevel of the atoms, $g_F = [F(F+1) + S(S+1) - I(I+1)]/[F(F+1)]$, I_S is the saturation intensity, defined as $I_S = 2\pi^2\hbar c\gamma/(3\lambda^3)$, and I_0 is the peak intensity $2P/(\pi w_0^2)$ in terms of the laser power P [12]. The detunings $\delta_{1/2}$ and $\delta_{3/2}$ (in units of γ) represent the difference between the laser frequency and the D_1 and D_2 transition frequencies, respectively. For Rb, $\gamma = 2\pi \times 6.1$ MHz.

The second term on the right hand side of Eq. (2) describes the optical Zeeman splitting [14] in terms of the ellipticity ϵ of the light polarization [15]. In this paper we mainly focus on linearly polarized trapping light, i.e., $\epsilon = 1$. However, in Sec. IV G we discuss how the loading of the FORT is affected when optical Zeeman splittings are present due to elliptical polarization of the FORT light.

III. EXPERIMENT

The experimental setup is schematically shown in Fig. 2. The starting point of all the experiments described here is a MOT, which collects ^{85}Rb atoms from a 5×10^{-10} Torr vapor and contains a maximum of about 3×10^8 atoms in steady state with a filling time constant of ≈ 12 s. Two extended-cavity diode lasers, both stabilized to atomic lines in ^{85}Rb at 780 nm with a dichroic atomic vapor laser lock [16] are used for the MOT. One laser provides 6 mW for trapping and cooling (divided between three retro-reflected beams) and is tuned red of the $5\,^2S_{1/2}\,F=3\rightarrow 5\,^2P_{3/2}\,F'=4$ transition by an amount denoted as Δ_M. We refer to this light as the ''primary'' MOT light, and denote its total six-beam intensity by I_M. The beams have a Gaussian beam radius of 9.3 mm. The other MOT laser is used for hyperfine

repumping and is tuned near the $5\,^2S_{1/2}F=2\rightarrow5\,^2P_{3/2}F'$ $=3$ transition. We refer to this light as the ''repump'' light, and denote its detuning as Δ_R ($\Delta_R=0$ unless otherwise indicated). We use one single retroreflected beam of intensity $I_R=3$ mW/cm^2 for repumping the MOT. Both laser beams have acousto-optic modulators (AOMs) in them for temporal control of the light intensity. The magnetic field gradient of the quadrupole field along the strong axis is 5 G/cm, and can be switched off within 3 ms.

The FORT light is generated with a home-built titanium-sapphire laser, with a nominal output power of 1.2 W. After passing through an AOM, the first order is intensity stabilized, collimated, and expanded. The beam is focused into the vacuum chamber with a 20 cm focal length doublet lens to a focus of radius $w_0=26$ μm ($1/e^2$ intensity), unless stated otherwise. The detuning from the D_2 line is typically 2 to 4 nm to the red. For $P=300$ mW, $w_0=26$ μm, and λ $=784$ nm the well depth $U_0/k_B=-1.4$ mK. Approximating the center region of the FORT potential as harmonic, the trap oscillation frequencies are 4.6 kHz and 34 Hz in the transverse and longitudinal directions, respectively. Note that the trap as a whole is highly anharmonic at the edges. The peak photon scattering rate for these parameters is 1.3 kHz.

Loading and diagnostics

The sequence for loading the FORT from the MOT and measuring the number of atoms is as follows. The MOT fills for typically 3 s at an optimum detuning of $\Delta_M\approx-2\gamma$, and at maximum repump intensity. This results in typically 3 $\times10^7$ atoms in the MOT. We then switch on the FORT while simultaneously increasing the detuning of the primary MOT light and reducing the repump light intensity. We will refer to this stage in the timing cycle as the ''FORT loading stage,'' which is typically 20–200 ms long, depending on FORT parameters. The primary MOT light, MOT repump light, and magnetic fields are switched off, and the atoms are held in the FORT for a variable length of time, but at least 100 ms, before the detection light comes on, so that the MOT cloud can fall out of the detection region. The atoms are then released from the FORT and detected by turning on the MOT light (primary and repump) but no magnetic field, with the primary MOT light frequency now closer to resonance $\Delta_M\approx-\gamma/2$. The number of atoms N is determined from the amount of fluorescence [17] collected with a low noise photodiode. Under some circumstances, the cloud of atoms trapped in the FORT is so large that it extends beyond the field of view of our photodetector. In this case the number is measured by recapturing them into a MOT. For this case the detection must be delayed for at least 250 ms to give the MOT cloud time to fall out of the MOT beams.

The number of atoms in the FORT is measured as a function of storage time. We call this a lifetime curve. A typical example of a lifetime curve is shown in Fig. 3. Note that the number of atoms does not have a simple exponential dependence on time. We find that the loss of atoms is well described by
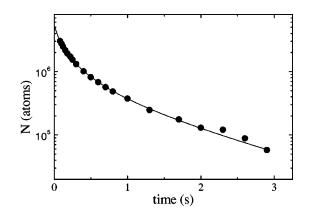

FIG. 3. Number of atoms remaining in the FORT as a function of time, for trap parameters $w_0=26$ μm, $P=290$ mW, λ $=782.5$ nm. The trap depth is $U_0/k_B=-2.3$ mK. The solid curve is a fit of Eq. (3) to the data.

$$\frac{dN}{dt}=-\Gamma N-\beta'N^2, \tag{3}$$

with Γ an exponential loss rate and β' a collisional loss coefficient. We use the analytical solution of Eq. (3) as a fit function to the data to find the number N_0 initially trapped, as well as values of Γ and β' (see Sec. VI). The prime on β' is used to refer to atom number loss instead of density loss.

We use absorption imaging to measure the size and temperature of the MOT cloud as well as the cloud of atoms in the FORT. Our imaging system consists of a two-lens telescope making a one-to-one image onto a charge-coupled-device (CCD) array. The lenses are 18 cm focal length cemented doublets. The line of view is perpendicular to the FORT beam. This allows us to observe the transverse as well as longitudinal shape of the cloud of atoms trapped in the FORT.

IV. DYNAMICS OF THE LOADING PROCESS

In Fig. 1 we showed that the transfer of atoms from the MOT to the FORT is a dynamical process, in which the number of atoms loaded into the FORT increases rapidly until a competing process causes the number to reach a maximum and then decrease at later times. Here we investigate the precise shape of the loading curve in more detail. The number of atoms in the FORT for longer loading times is shown in Fig. 4.

The shape of the loading curve is explained as follows. Initially, the number of atoms in the FORT increases as $N(t)=R_0t$. But at larger times the number starts to roll over. This occurs for two reasons. First, the MOT loses atoms due to the reduced repump intensity and different detuning of the primary MOT light. This reduces the loading rate. Second, the trap loss rates become large enough to counteract the loading.

Similarly to Eq. (3) we find that the shape of the FORT loading curve is well described by

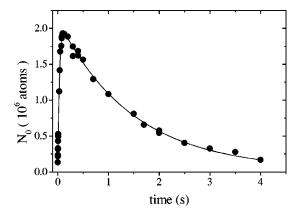$$\frac{dN}{dt}=R_0\exp(-\gamma_{MOT}t)-\Gamma_LN-\beta'_LN^2, \tag{4}$$

FIG. 4. Number of atoms loaded in the FORT as a function of FORT loading stage duration, for trap parameters $w_0 = 26$ μm, $P = 305$ mW, and $\lambda = 784.5$ nm. Primary MOT intensity $I_M = 8.2$ mW/cm^2 and MOT repump intensity $I_R = 4.7$ μW/cm^2. The solid curve is a fit of Eq. (4) to the data. The loss coefficient $\beta'_L = (1.56 \pm 0.22) \times 10^{-5} (\text{atoms s})^{-1}$; see text.

where γ_{MOT} is the rate at which the MOT loses atoms due to the change of MOT light detuning and repump intensity, and Γ_L and β'_L characterize density independent and density dependent losses. The subscript ''L'' expresses the fact that the loss rates during loading are generally different from those during storage in the FORT without any MOT light present.

Four parameters determine the loading: R_0, γ_{MOT}, Γ_L, and β'_L. To understand the physics of the loading process we must therefore determine these four parameters under a variety of conditions. The initial loading rate R_0 can be determined directly from the initial slope of the loading curve. Then γ_{MOT} can be determined by measuring the rate at which the MOT fluorescence decreases during the FORT loading stage. We confirmed this explicitly by allowing the MOT to dissipate for a variable length of time τ_d before the start of the FORT loading stage. The initial slope of the loading curve $R(\tau_d)$ was observed to be $R(\tau_d) = R_0 \exp(-\gamma_{MOT}\tau_d)$, consistent with the MOT fluorescence measurement. The rate constants β'_L and Γ_L can then be determined by fitting the numerical solution of Eq. (4) to the data. The solid curve in Fig. 4 is such a fit, indicating how well the loading process is described by Eq. (4). With R_0 and γ_{MOT} constrained to the directly measured values, as mentioned above, the extracted values of β'_L and Γ_L show that the $-\beta'_L N^2$ loss term clearly dominates over the $-\Gamma_L N$ term. This is most apparent in the slope of the tail of the load curve. Thus, collisional processes dominate the losses from the FORT during its loading.

The losses during the loading of the FORT can be studied independently from the loading rate. This is done as follows. The FORT is first loaded under optimum conditions, and the atoms are stored for 100 ms, after which the MOT lasers are switched back on, with no magnetic field, for the remainder of the FORT storage time. At the end of this cycle, we detect the number of atoms remaining in the FORT. We refer to such a measurement as a loss curve measurement. In this way we can study the effect of the MOT light field parameters on the loss rate; i.e., we have eliminated the loading
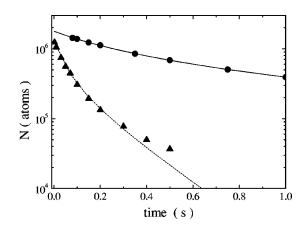

FIG. 5. Number of atoms in the FORT vs time, without any MOT light (●) and with MOT light on (▲); primary MOT intensity $I_M = 8.2$ mW/cm^2, and MOT repump intensity $I_R = 4.7$ μW/cm^2, for trap parameters $w_0 = 26$ μm, $P = 305$ mW, and $\lambda = 784.5$ nm. The curves are fits of Eq. (3) to the data. The number dependent loss rates are $\beta' = (1.42 \pm 0.05) \times 10^{-6} (\text{atoms s})^{-1}$ and $\beta'_L = (1.4 \pm 0.1) \times 10^{-5} (\text{atoms s})^{-1}$, for the atoms stored in the FORT without any MOT and with MOT light, respectively.

term in Eq. (4). With the MOT lasers on, the loss rate is much larger than in the absence of any MOT light and completely dominated by density dependent losses β'_L. The result of such a measurement is shown in Fig. 5 (▲), which also contains the lifetime curve (●) recorded in the absence of MOT light. Comparing corresponding loading and loss curves we find the same values of β'_L from the different types of data sets to within a 30% spread. The advantage of measuring a loss curve is that we can independently change all the MOT light field parameters without altering the number of atoms initially loaded into the FORT.

The nice agreement between the value of β'_L determined from the loading curve in Fig. 4 and the loss curve in Fig. 5, taken for identical MOT and FORT parameters, gives good confidence that Eq. (4) describes the physics involved in loading the FORT.

The fact that collisional losses, β'_L, dominate the tail of the loading curve can also be seen in another way. If one neglects the $-\Gamma_L N$ term in Eq. (4) and sets the loading rate to be constant at R_0, i.e., assuming that the MOT does not lose atoms during the loading of the FORT, the steady state solution of Eq. (4) is

$$N_{st} = \sqrt{R_0 / \beta'_L}. \qquad (5)$$

Substituting the values of R_0 and β'_L obtained as discussed above, the calculated N_{st} agrees to within 10% with the maxima of the loading curve.

We did some extra checks on the accuracy of fitting Eq. (4) to the data. One test was to set all four parameters in Eq. (4) free. This reproduced the independently determined values of R_0 and γ_{MOT}, as well as those of Γ_L and β'_L, with Γ_L the least well determined. Both γ_{MOT} and Γ_L give rise to exponential decay and are therefore strongly coupled in the
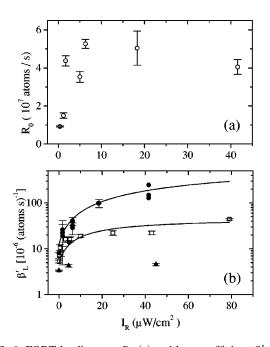
FIG. 6. FORT loading rate R_0 (a) and loss coefficient β'_L (b) as a function of hyperfine repump light intensity, for trap parameters $w_0 = 26$ μm, $P = 300$ mW, and $\lambda = 784.5$ nm. The loss rate was measured for $I_M = 8$ mW/cm^2 ($\bullet$), reduced MOT intensity of $I_M = 1$ mW/cm^2 ($\square$), and complete absence of primary MOT light ($\blacktriangle$). The solid curves are fits to the data based on the model described in Sec. VII A. Error bars are statistical and do not reflect systematic uncertainties in I_M.

least squares fit. Most often, we find that the fit determines a Γ_L within error of zero and a γ_{MOT} within 20% of the value determined directly from the MOT fluorescence. Assuming that the value of Γ_L should at least be as big as that of the trap in the absence of the MOT light, we set it to that value and see no significant change in the value of β'_L. Fitting the loading curves with these constraints and different combinations of free parameters, we find a spread in the β'_L values of up to 30% for a given data set, which is more than adequate for the analysis given below. We are now in a position to investigate the loading of the FORT in terms of R_0 and β'_L separately, by measuring either load curves or loss curves.

A. Hyperfine repump intensity and detuning

A commonly used technique to improve the loading of a FORT is to reduce the hyperfine repump intensity. Here we show how the intensity and detuning of the repump light affect the loading rate R_0 as well as the loss rate β'_L. We concentrate first on the dependence of the loading rate and loss rate on the hyperfine repump intensity at resonance ($F = 2 \rightarrow F' = 3$). The data in Fig. 6 show that for the maximum I_M there is a critical repump intensity below which the MOT is not sustained during the FORT loading stage and the loading rate goes to zero. For I_R above that critical value, the loading rate decreases slightly because the density in the MOT decreases due to radiative repulsion. The optimum level is about $I_R = 5$ μW/cm^2. Note that the loading rate of the FORT is as high as 5×10^7 atoms s^{-1}, which is a factor
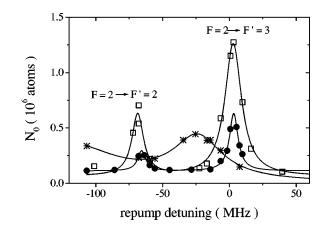

FIG. 7. Number of atoms in FORT as a function of MOT hyperfine repump detuning for different repump intensities, 1.4 μW/cm^2 ($\bullet$), 4 μW/cm^2 ($\square$), and 280 μW/cm^2 (*). FORT parameters are $w_0 = 26$ μm, $P = 200$ mW, and $\lambda = 798.1$ nm. Solid curves are Lorentzians fitted to the data to guide the eye. Detuning is relative to the unperturbed $F = 2 \rightarrow F' = 3$ repump transition.

2 higher than that of our MOT. The loss rate β'_L increases rapidly with repump intensity and starts to saturate at high repump intensity. For lower I_M, saturation sets in at lower repump intensities and β'_L is smaller.

The optimum repump intensity is intimately linked to the repump detuning. This interdependence is shown in Fig. 7, where the maximum number of atoms loaded into the FORT is plotted versus Δ_R for different values of I_R. Increasing I_R from 1.4 μW/cm^2 to 4 μW/cm^2, we see that the number in the trap increases, but the optimum repump detuning stays on resonance. Increasing the intensity to 280 μW/cm^2 causes the optimum repump detuning to redshift. Interestingly, the optimum number of atoms is loaded when the repump scattering rate is the same for both $I_R = 4$ μW/cm^2 and $I_R = 280$ μW/cm^2 due to the different detuning, indicating that an optimum repump scattering rate exists for loading the FORT. However, the number of atoms drops and the resonance broadens, which shows that the number of atoms in the FORT is not determined by the repump scattering rate alone. This will be explained in more detail in Sec. VIII.

In summary, the loading rate R_0 is optimal for a very low repump intensity of about 5 μW/cm^2 and zero detuning. The loss rate β'_L increases with repump intensity and is larger for higher intensity of the primary MOT light.

B. Primary MOT light intensity

Both R_0 and β'_L depend on the primary MOT intensity I_M. The data in Fig. 8 show that β'_L rises rapidly and then saturates with increasing I_M. The MOT intensity at which saturation sets in is higher for higher repump intensities. Combined with the dependence of β'_L on repump intensity, this suggests that excited state collisions leading to radiative escape are responsible for the losses during loading, as is confirmed by the model that we develop in Sec. VII. The solid curves in Figs. 6(b) and 8(b) are based on this model and agree very well with our data.
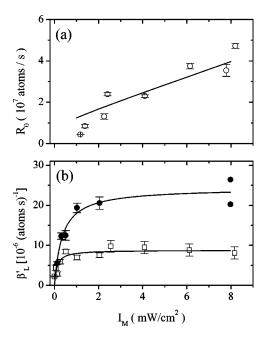
FIG. 8. FORT loading rate R_0 for a repump intensity of 5 μW/cm^2 (a) and loss coefficient β_L' (b) as a function of primary MOT light intensity, where β_L' was measured for zero repump intensity ($\square$) and $I_R = 5$ μW/cm^2 ($\bullet$). The solid curve in (a) is derived from the model described in Sec. VII B. The solid curves in (b) are fits to the data of the model described in Sec. VII A. FORT parameters as in Fig. 6.

As shown in Fig. 8, the loading rate R_0 increases nearly linearly with I_M. As will be argued in Sec. VII, this implies that the loading rate strongly depends on the cooling mechanisms in the MOT.

C. Role of MOT detuning

Both R_0 and β_L' depend also on MOT detuning, as shown in Fig. 9. For these data, I_R is reduced to the value that gives optimum loading into the FORT. A maximum in R_0 is observed at about $\Delta_M \approx -30$ MHz. At slightly larger detuning the loss rate β_L' has a minimum. The maximum number of atoms is loaded into the FORT at a detuning close to the maximum in the loading rate and simultaneous minimum in the loss rate.

We also observe that the optimum detuning of the primary MOT light during the loading stage depends on the depth of the FORT. This is illustrated in Fig. 10. For deeper traps, the optimum detuning is smaller. The FORT depth was varied by changing the wavelength and power of the FORT light.

D. Role of the magnetic field gradient

In order to determine the influence of the MOT magnetic field gradient, we measured R_0 and N_0 for different currents in the MOT coils during the FORT loading stage. We find R_0 to be nearly independent of the magnetic field gradient in the range from 1.5 to 17.5 G/cm. At very small or very large gradients, however, atoms are rapidly lost from the MOT during the FORT loading stage, which strongly reduces N_0
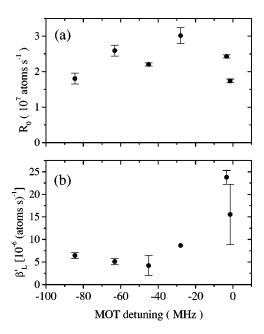

FIG. 9. FORT loading rate R_0 (a) and loss coefficient β_L' (b) as a function of the primary MOT light detuning Δ_M during loading. The repump intensity is 5 μW/cm^2. For trap parameters $w_0 = 26$ μm, $P = 300$ mW, and $\lambda = 784.5$ nm.

because it shortens the effective loading time. At intermediate gradients, in the range from 3.5 to 12.0 G/cm, the losses from the MOT are small, with the maximum number loaded near 5.0 G/cm.

E. Alignment with respect to the MOT

Another factor affecting the FORT loading is the relative alignment of the FORT with respect to the MOT. We find that the loading rate is optimum with a longitudinal displacement between the center of the FORT and the MOT. The optimum displacement depends on the FORT depth. Absorption imaging is used to determine the separation between the FORT and the MOT. We observe that the displacement for which the loading rate is optimized increases with trap depth. Typically the displacement between the focus of the FORT and the MOT is about one-half a MOT diameter.
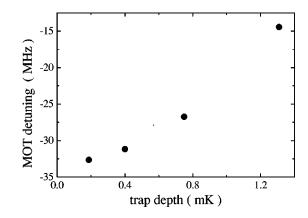

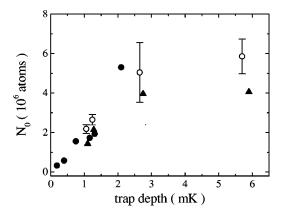FIG. 10. MOT detuning for maximum number of atoms loaded into the FORT versus trap depth, $w_0 = 26$ μm.

FIG. 11. Number of atoms loaded into the FORT as a function of trap depth for $w_0 = 26$ μm ($\bullet$) and $w_0 = 22$ μm ($\blacktriangle$). For the latter data set, the steady state number [see Eq. (5)] is calculated from R_0 and β_L' (taken from Fig. 12 below) and plotted as $\bigcirc$.

In shallower traps the displaced loading of the atoms causes an initial sloshing of the atoms in the longitudinal direction. The sample of atoms can be seen to make one and one-half oscillations before it thermalizes at the center of the FORT; this takes about 100 ms.

F. Dependence on FORT depth

We measured how the loading rate, loss rate, and total number of atoms trapped in the FORT depends on the trap depth. This is shown in Figs. 11 and 12. For each data point, the MOT detuning, repump intensity, and alignment of the FORT with respect to the MOT were optimized to give the highest number of atoms in the FORT. The primary MOT light intensity was fixed at the highest available value of 8 mW/cm^2, which optimizes the loading rate (see Sec. IV B). The waist of the trapping beam is fixed, and the trap
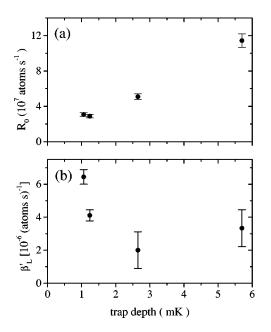

FIG. 12. FORT Loading rate R_0 (a) and loss rate β_L' (b) as a function of trap depth U_0 for $w_0 = 26$ μm.
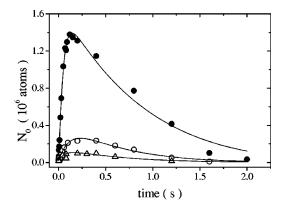

FIG. 13. Number of atoms in the FORT as a function of loading time for three different ellipticities of the FORT light. In descending order of the curves, $\epsilon = 0.999$, 0.915, and 0.852. The FORT parameters are $w_0 = 22$ μm, $P = 600$ mW, and $\lambda = 784.5$ nm.

depth is varied by changing both the detuning and power of the FORT beam. The dependence of N_0 on trap depth can be explained as an increase in R_0 and a reduction of β_L' as the trap gets deeper. This is illustrated by the data shown in Fig. 12.

For comparison to the data in Fig. 11, we calculated N_{st} using Eq. (5) by inserting the measured R_0 and β_L'. The calculated values N_{st} ($\bigcirc$ in Fig. 11) agree well with the measured number and depend linearly on trap depth up to 3 mK. At 6 mK, N_0 lies below the extrapolated straight line because β_L' cannot decrease below the value obtained in the absence of MOT light.

For a waist of 26 μm, we have observed transfer efficiencies from the MOT to the FORT of 20%. For traps with a larger waist, $w_0 = 40$ μm, transfer efficiencies of 40% and higher have been observed. If we compare FORTs with about the same depth of $U_0 \approx -1$ mK but different waists, we observe that more atoms are loaded when the waist is bigger. This is mainly due to an increase of the loading rate (see Sec. VII B). Changing the waist from 26 μm to 75 μm, we observed a strong reduction of the lifetime of the trapped sample. We could attribute this reduction to the fact that the scattering force became stronger than the trapping force [1].

G. Effect of elliptically polarized FORT light

As the data in Fig. 13 show, the polarization of the FORT light has a profound effect on the number of atoms loaded into the FORT. A change of the ellipticity [15] from linear polarization, $\epsilon = 0.999$, to slightly elliptical polarization, $\epsilon = 0.915$, causes the number of atoms to drop by a factor of 7. At $\epsilon = 0.852$ the number dropped by more than an order of magnitude. The drop in number is caused by a combination of effects. Analysis of the shape of the load curves in Fig. 13 shows that the loading rate is reduced by an order of magnitude and the exponential loss rate Γ_L is increased by a factor of 4. The increase of Γ_L we ascribe to the ground state dipole force fluctuations related to the optical Zeeman splittings [second term on the right hand side of Eq. (2)] induced by the ellipticity of the light [18]. The optical Zeeman splittings
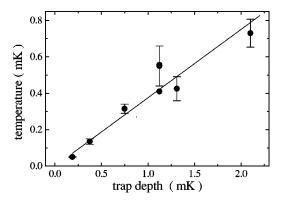
FIG. 14. Temperature of the atoms in the FORT as a function of trap depth, for $w_0 = 26$ μm. Solid line is a linear regression giving a slope $T/|U_0| = 0.4$.

can also be expected to interfere with the functioning of the MOT and thus reduce the loading rate. In the center of the FORT, the splitting corresponds to that of a magnetic field of 13 G. Although our MOT operates in the sub-Doppler regime, these large splittings disrupt even the Doppler cooling and trapping mechanisms of the MOT, which we believe are mainly responsible for loading of the FORT.

V. TEMPERATURE

We measured the temperature of the atoms in the FORT for different trap depths. The temperature T of the atoms in the FORT was determined from the rate at which the cloud of trapped atoms expands after release. The density distribution is well described by a Gaussian of width σ that increases upon expansion as $\sqrt{\sigma_0^2 + (k_B T/m) t^2}$. For the data shown in Fig. 14 we used the expansion in the transverse direction to obtain T. The initial aspect ratio of the cloud is 33 to 3000 μm. We confirmed that within experimental uncertainties the temperatures in the transverse and longitudinal directions are the same. Note that for the deeper traps the temperature is much higher than that of the atoms in the MOT, which is about 30 μK to 120 μK, depending on the MOT detuning. Over the range of trap depths that we investigated the temperature is a fixed fraction 0.4 of the FORT depth.

VI. TRAP LIFETIME

The number of atoms in the trap decreases after the trap is loaded, as shown in Fig. 3. In the absence of any MOT light, the loss of the trapped sample has a number dependent (collisional) portion and a purely exponential part, as described by Eq. (3).

Typically, the exponential lifetime $1/\Gamma$ is between 1 s and 10 s, depending on the trap parameters. The lifetime increases with decreasing FORT scattering rate, until a limit (≈ 10 s) is reached that we believe is set by the background vapor pressure.

The collisional loss, characterized by β', depends on the wavelength and waist size of the FORT beam. We observe clear resonances in β', consistent with photoassociation lines. Between these lines, we see a nonzero background

level that presumably is due to ground state hyperfine changing collisions. This background level depends on the FORT light polarization. In a circularly polarized FORT [18], the atoms are spin polarized in one of the stretched states of the $F=3$ ground state, from which hyperfine changing collisions are suppressed. In our trap, we see a factor of 2 reduction of β' in between the photoassociation lines when the polarization is changed from linear to circular.

VII. ANALYSIS

A. Analysis of density dependent losses

The main features that we have observed in our data are the strong increase ($\times 100$) of the collisional loss coefficient β'_L when the MOT light is present and the strong dependence of this loss rate on the MOT parameters. As we will show in this section, density dependent losses during the loading of the FORT are mainly due to radiative escape collisions induced by the MOT light. In the unperturbed FORT, ground state hyperfine changing collisions are the dominant loss process.

1. Conversion to density dependent loss

The typical mechanism driving the collisional loss process in the FORT is more easily identified when the measured rate coefficients β' and β'_L are converted to density related, volume independent rate coefficients β and β_L. The relation between these is $\beta = \beta' V$, with V the volume of the sample of atoms. The volume is found by approximating the trapped sample of atoms as a cylinder with radius and length determined by the size of the FORT beam focus and the temperature of the atoms. The volume is then given by

$$V = \pi w_0^2 z_R \ln\left(\frac{1}{1-\eta}\right) \sqrt{\frac{\eta}{1-\eta}}, \tag{6}$$

where $\eta = k_B T/|U_0|$ is shown in Sec. V to be a constant 0.4, regardless of the FORT parameters. Thus the volume changes only when w_0 changes.

2. Density dependent loss from the FORT without the MOT present

Density dependent losses from the FORT when there is no MOT light present are due to both photoassociation and ground state hyperfine changing collisions, as mentioned in Sec. VI. Between photoassociation lines, the values of β' do not depend strongly on the FORT laser power or wavelength, but change strongly with the trap volume V. Note that, because $z_R \propto w_0^2$, $V \propto w_0^4$. However, the resulting $\beta = \beta' V = (4 \pm 2) \times 10^{-12}$ cm^3 s^{-1}, for waists ranging from 25 μm to 58 μm. This value of β agrees well with the value of 4×10^{-12} cm^3 s^{-1} reported by Miller [19].

3. Density dependent loss from the FORT during loading

In the case of loading the FORT, the density dependent losses are due to light-assisted collisions. To demonstrate this, we compare them with measured rates in MOTs, where light-assisted collisions have been extensively studied. This

comparison is complicated by the difference in trap depth between the MOT and the FORT (1 K vs 1 mK) and also the difference in fractional occupation of the upper hyperfine component of the ground state. In the case of the MOT, the fractional population of the lower hyperfine component is negligible, and the loss term is written as βn^2, where n is the total density of atoms in the MOT. In general, β depends linearly on the intensity of the assisting light.

These light-assisted collisions, as described by Gallagher and Pritchard [20], are due to two mechanisms: fine structure changing collisions and radiative escape. It has been shown that these two mechanisms contribute with the same order of magnitude to the trap loss [21,22] in 1 K deep MOTs. Radiative escape is predicted to scale almost inversely with trap depth ($\beta \sim U_0^{-5/6}$) [22,23] for trap depths $\sim$ 1 K, but the fractional contribution of fine structure changing collisions should decrease with decreasing trap depth. Therefore, we can neglect the contribution from fine structure changing collisions to β in describing the losses that occur during loading of the 1 mK deep FORT.

The fractional ground state population affects the loss rate in the following way. For radiative escape to occur, at least one of the two colliding atoms must be in the upper hyperfine ground state ($F = 3$). The MOT light is too far detuned to excite an atom from the lower ground state ($F = 2$) to a higher lying molecular state during a collision. Therefore, the loss term takes the form of $\beta n_3(n_2 + n_3)$, where n_3 is the density of atoms in the $F = 3$ state, n_2 is the density of atoms in the $F = 2$ state, and $n_2 + n_3 = n$.

The fraction of atoms in the $F = 3$ state depends on the relative optical pumping rates of the primary MOT laser ($F = 3 \rightarrow F' = 3 \rightarrow F = 2$) as compared with the repump laser ($F = 2 \rightarrow F' = 3 \rightarrow F = 3$). We derive the fraction of atoms in the $F = 3$ state from a simple two-level rate equation model, which results in $n_3/n = I_R/(I_R + a I_M)$, where a is a constant that reflects the relative optical pumping rates. These rates depend on the ac Stark shifts induced by the FORT, in addition to Clebsch-Gordan coefficients and the frequency of each laser. The average shift in the transition frequency for atoms in the FORT (Δ_{ac}) was extracted from Fig. 7 and found to be $\Delta_{ac} = 2.3\gamma$. This results in $a = 0.02$. The experimentally determined loss rate coefficient is then

$$\beta'_L = \frac{K I_M}{V} \frac{I_R}{I_R + a I_M}, \tag{7}$$

where K is a constant related to the density dependent loss rate, independent of optical pumping effects. We again use the volume V given by Eq. (6) to make the translation from the typical density dependent loss rate to the loss coefficient that we measure in our experiments. For $w_0 = 26$ μm, we find $V = 1.3 \times 10^{-6}$ cm^3.

The behavior described by Eq. (7) is clearly seen in the measured dependence of β'_L on both I_M and I_R as shown in Figs. 6(b) and 8(b). The solid curves in these plots are fits of Eq. (7) to the data, with K the only free parameter. The fits to the different data sets give $K = (1.1 \pm 0.5) \times 10^{-10}$ cm^5 mW^{-1} s^{-1}, where the spread is due to the different values we find by fitting different data sets taken on
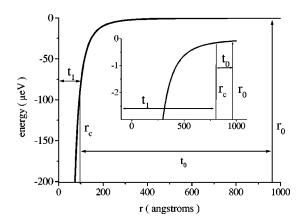

FIG. 15. Approximate intramolecular potential for Rb, with $C_3 = 71$ Å^3 eV. The large graph shows the critical radius r_c for $U_0/k_B = -1$ K, while the inset depicts the same parameters for $U_0/k_B = -1$ mK.

different days. We see that Eq. (7) gives a good description of the measured MOT and repump intensity dependences of the loss rate during loading of the FORT.

For a comparison of our numbers with those normally found in MOTs we set $n_3/n = 1$, assuming all atoms are in the $F = 3$ ground state as they would be in a MOT. Thus $\beta_L = K I_M$. For $I_M = 10$ mW/cm^2 we find $\beta_L = 1 \times 10^{-9}$ cm^3/s. In contrast, a MOT with comparable powers and detunings has a loss rate of $(1-4) \times 10^{-12}$ cm^3/s [24–26,23], which is a factor of 250 to 1000 smaller than our measured value. As shown below, this difference is due to the smaller depth of the FORT.

In order to explain the increased loss rate observed during loading of the FORT as compared to a MOT, we will discuss in more detail how the FORT depth affects the radiative escape loss rate. In the case of a MOT, the dependence of β, due to radiative escape, on the trap depth is predicted to vary as $U_0^{-5/6}$ in the limit of large trap depths [22,23]. However, some of the assumptions used to derive this dependence break down at smaller trap depths. Therefore, to calculate β_L for the FORT, we perform a numerical calculation of the radiative escape process, using the semiclassical Gallagher-Pritchard (GP) model [20]. Given the uncertainties in our measured β_L, a more detailed calculation is unwarranted. Therefore, we do not include angular momentum considerations or enhanced survival probability as described by Julienne and Vigue [22] or any corrections for the hyperfine splittings as introduced by Lett *et al.* [21]. Instead, we approximate all of the involved intramolecular potentials as a single $-C_3/r^3$ in the GP model, as formulated by Peters *et al.* [27], and integrate numerically.

Figure 15 shows an approximate intramolecular potential for Rb. For initial excitation at radius r_0, atoms are accelerated toward one another for some time before spontaneous emission leaves two ground state atoms with more kinetic energy than they had initially. If the kinetic energy picked up in the collision exceeds the depth of the trap, both atoms will be lost. The radius at which the pair acquires exactly enough energy to be ejected from the trap is therefore called the critical radius r_c, and the time required for the atoms to reach this is called t_0.
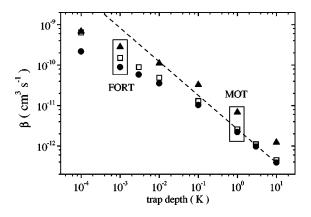
FIG. 16. Radiative escape loss rate coefficient β calculated as a function of trap depth. When the atoms have zero initial kinetic energy, ▲ correspond to β values for $\Delta_{AC}+\Delta_M=2\gamma$ and ● to 8γ. □ depict 8γ, but with an initial relative velocity $v=k_BT/m$, corresponding to $T=800$ μK. The dashed line represents $\beta\propto U_0^{-5/6}$ as mentioned in the text.

Once the atoms reach r_c, acceleration is very fast, and the atom pair spends a short time t_1 accelerating to $r=0$. If spontaneous emission does not occur during this second time interval, the intramolecular separation will oscillate between 0 and r_0, making multiple orbits until spontaneous emission occurs. The probability of a lossy radiative escape event thus depends on the excitation probability at r_0 and the probability of decay occurring when $r<r_c$. Following Refs. [27] and [28] we find

$$\beta\propto\int 4\pi r_0^2 dr_0 G(r_0)P_{RE}(r_0),\qquad(8)$$

where the photon scattering rate of atoms in the $F=3$ state, $G(r_0)$, is a function of the effective detuning $\Delta(r_0)=-C_3/(r_0^3\hbar)+\Delta_M$ with respect to the unperturbed atomic transition frequency. The probability of a radiative escape event resulting in trap loss is $P_{RE}=\sinh(\gamma t_1)/\sinh[\gamma(t_0+t_1)]$, which reflects the important contribution of multiple orbits [27].

The result of the numerical integration of Eq. (8) for different trap depths is shown in Fig. 16. The dashed line indicates a dependence of $\beta\sim U_0^{-5/6}$ as predicted by Refs. [22] and [23]. This clearly tracks our numerical integration at large trap depths, where it is expected to be valid. Examination of the change in β with U_0 shows that for a change in U_0 from -1 K to -1 mK, β increases by a factor of ~50 (for $n_3/n=1$). This ratio is at least a factor of 5 smaller than the experimentally observed ratio of 250. However, given the large uncertainties in the experimental determination of n and n_3/n, as well as the approximations that go into the calculations and the steep dependence of the results, the measured and calculated numbers are not inconsistent. Therefore, we believe that the enhanced loss rates we observe during loading are consistent with light-assisted collisions.
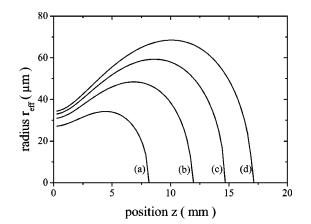

FIG. 17. Equipotential contours of the FORT for $U_c/k_B=-100$ μK, $U_0/k_B=-1$, -2, -3, and -4 mK depth, (a)–(d), and $w_0=26$ μm.

B. A model for the FORT loading rate

The initial loading rate is the flux of atoms into the volume of the FORT times the probability for an atom in this volume to become trapped:

$$R_0=\tfrac{1}{4}n_{MOT}\bar{v}AP_{trap},\qquad(9)$$

where n_{MOT} is the density in the center of the MOT, $\bar{v}=\sqrt{k_BT/m}$ is the root mean square velocity of the atoms in the MOT, A is the effective surface area of the FORT, and P_{trap} is the trapping probability. For the discussion below, we will assume that the MOT density is constant, i.e., n_{MOT} is the density at the start of the loading stage.

As was shown in Fig. 9, R_0 has a maximum at $\Delta_M=-30$ MHz. At the same detuning, the measured product $n_{MOT}\sqrt{T_{MOT}}$ has a maximum. This supports the idea that $R_0\propto n_{MOT}\bar{v}$.

In addition to n_{MOT} and $\bar{v}$, the loading rate R_0 also depends on A. For a trap with a waist of 26 μm, the Rayleigh range is 2.7 mm. This is about 5 times larger than the diameter D_{MOT} of the cloud of atoms trapped in the MOT. This means that the FORT radius hardly changes over a distance D_{MOT}. Therefore we approximate A by the surface area of a cylinder with length D_{MOT} and an effective radius r_{eff} that depends on the relative longitudinal position of the MOT with respect to the FORT. The radius is set by the position on the FORT potential where it becomes significant compared to the temperature of the atoms in the MOT, $U(r_{eff},z)=U_c\approx-k_BT$. The effective radius $r_{eff}(z)$ of the FORT, depending on z and U_c, is then

$$r_{eff}(z)=\left[\frac{w_0^2}{2}[1+(z/z_R)^2]\ln\left(\frac{U_0}{U_c}\frac{1}{1+(z/z_R)^2}\right)\right]^{1/2}.\qquad(10)$$

In Fig. 17 this equipotential contour is plotted for different values of U_0 and $U(r_{eff},z)=-100$ μK. The bow tie shape of these contours explains why the best loading is achieved when the FORT and MOT are displaced; the radius has a maximum away from the focus. Moreover, for deeper traps,

the z at which the maximum radius occurs shifts to larger z values, just as in the loading data.

A typical initial MOT density during the FORT loading stage is 2×10^{11} cm^{-3}, and the temperature ranges from 30 μK to 100 μK, depending on detuning of the primary MOT light. A reasonable value for the average speed in one dimension is thus $\bar{v} = 5$ cm/s. The MOT diameter is 500 μm (full width at half maximum). For $U_0/k_B = -1$ mK and $U_c/k_B = -100$ μK the area $A = 1 \times 10^{-3}$ cm^2. Using these numbers, the loading rate is 2.5×10^8 s^{-1} if the trapping probability $P_{\text{trap}} = 1$. The loading rate measured for such a trap is 3×10^7 s^{-1}, implying $P_{\text{trap}} \approx 0.1$.

The data in Fig. 8 show that the loading rate increases nearly linearly with MOT intensity. However, it is known that the MOT temperature and density in the sub-Doppler regime scale as intensity and the inverse square root of intensity, respectively [17,29]. The product $n_{\text{MOT}} \bar{v}$ is thus expected to show no strong dependence on MOT intensity. We have experimentally confirmed this by measuring the density and temperature of the cloud of MOT atoms as a function of MOT intensity. Over the range of MOT intensities as in Fig. 8, we find that $n_{\text{MOT}} \bar{v} A$ is nearly constant. Therefore, we conclude that the observed increase of the loading rate with increasing MOT intensity arises from an intensity dependence of the trapping probability P_{trap}.

We estimate P_{trap} by using the following simple model. The atoms come into the trapping volume with a narrow distribution of velocities around an average velocity $\bar{v}$. To be trapped, an atom's energy has to be reduced to below the edge of the trapping potential. The time scale for this to happen must be about one-half the oscillation period $\tau/2$ of the FORT in the strong direction, which is 150 μs for the above mentioned trap. The scattering of MOT laser photons affects the atomic velocity in two ways. First, the atom scatters photons, which leads to heating, that is, a broadening of its velocity distribution. The spread in velocity due to photon scattering is $\sigma = \sqrt{\frac{1}{3}(\hbar k/m)^2 \Gamma_{\text{scat}} \tau/2}$. Second, the frictional component of the scattering leads to a reduction of the atom's average kinetic energy. The rate at which the atom loses energy is $\dot{E} = -\alpha \bar{v}^2$, with α the friction coefficient. This damping leads to a change in average velocity of $\Delta v = \bar{v} \sqrt{\alpha \tau/m}$ in the characteristic time $\tau/2$.

The probability of being captured is the integral of the shifted and broadened distribution,

$$P_{\text{trap}} = \int_{\bar{v} - \Delta v}^{\infty} \frac{1}{\sqrt{2\pi}\sigma} \exp\left(-\frac{v^2}{2\sigma^2}\right) dv. \qquad (11)$$

The integral leads to

$$P_{\text{trap}} = \frac{1}{2} \left\{ 1 - \text{erf}\left[\frac{\bar{v}}{\sqrt{2}\sigma}\left(1 - \sqrt{\frac{\alpha\tau}{m}}\right) \right] \right\}. \qquad (12)$$

For $\Delta_M = 30$ MHz and $I_M = 6$ mW/cm^2 the MOT scattering rate $\Gamma_{\text{scat}} = 9.5 \times 10^5$ s^{-1}, which makes $\sigma = 6$ cm/s.

We obtain a value of α from the formula given in Ref. [23], based on Doppler cooling. The damping rate calculated from this formula increases linearly with MOT intensity for the velocities we are interested in. The values of α and σ also depend on MOT detuning. There is a strong spatial dependence of the effective MOT detuning due to the light shift induced by the FORT. We make the crude approximation that the MOT is shifted out of resonance by one-half the FORT light shift. This results in $\bar{v}/\sigma = 2$ and $\alpha/m = 200$ s^{-1}. The result of this model is plotted as a solid curve in Fig. 8 and shows good agreement with the data. This is a very approximate treatment, but it clearly supports our general interpretation of the loading process.

VIII. SUMMARY

From our understanding of the loss process and the loading rate, we are now in a position to explain the dependencies presented in Sec. IV. We saw that more atoms are loaded into deeper FORTs because the loading rate increases and the loss rate decreases. The loading rate increases because the effective FORT radius increases with trap depth, which enhances the flux of atoms into the trap. The loss rate decreases because the probability of light-assisted collisional loss decreases when the trap is deeper. In addition, the light shift of the trap increases the effective detuning of the MOT light and repump light for the atoms in the trap, which reduces their excitation rate, and therefore reduces radiative escape.

The data in Fig. 10 show that the MOT detuning at which loading is optimized is smaller for deeper FORTs. A deeper trap means larger light shifts of the atoms. The MOT detuning and the repump detuning are both blueshifted, so that the detuning of both lasers from the atoms becomes more negative (red) in both cases. Due to the increased effective detunings, the MOT cooling rate decreases, and the trapping probability thus decreases. By choosing a smaller MOT detuning the loading rate is increased.

The dependence on MOT detuning of the β_L' that we measured for a given trap depth (see Fig. 9) is also well described by Eq. (7). The detuning dependence enters through the parameter a. At small MOT detunings, the MOT excitation rate is highest, and β_L' is therefore large. By increasing the MOT detuning further, a becomes smaller. Therefore, $a I_M$ becomes negligible compared to I_R, and β_L' becomes independent of detuning.

In Sec. IV A, it was shown that loading is optimized for repump light of very low intensity that is tuned on resonance. We saw that the number of atoms in the FORT dropped when the repump intensity was increased, but the repump scattering rate was maintained by changing the repump detuning. Increasing the repump intensity increases the loss rate. Although the detuning is increased for the atoms in the MOT such that the scattering rate is the same for the MOT atoms, the increased intensity still causes an increased scattering rate for the atoms trapped in the FORT.
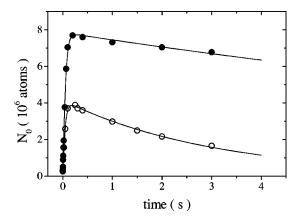
FIG. 18. Number of atoms loaded into the FORT as a function of loading time, using normal loading (○) and enhanced loading with a shadowed repump beam (●). The FORT parameters are $w_0 = 58$ μm, $P = 580$ mW, and $\lambda = 783.2$ nm. The solid curves are fits of Eq. (4) to the data.

IX. ENHANCED AND QUASICONTINUOUS LOADING

The previous data and analysis show that β_L' is very small when the repump power is zero, and reducing the primary MOT intensity also helps to reduce the loss rate. However, reducing these light intensities also reduces the loading rate. It is possible to improve the ratio of loss to loading rate by changing the beam geometry. The loss rate only has to be eliminated in the volume occupied by the FORT, which can be accomplished by inserting obstructions to block portions of the MOT and repump beams.

To demonstrate this concept, we make a shadow in the repump beam. For this purpose an additional repump beam is used that copropagates with the FORT beam. A 0.6 mm opaque disk in this beam is imaged into the MOT and FORT region, such that the shadow covers the length of the FORT. The peak intensity in this repump beam is increased from 5 μW/cm^2 to 460 μW/cm^2, which is sufficient to prevent the MOT from being lost while loading the FORT. The MOT is still loaded as before using a repump beam without a shadow. During the loading of the FORT, this repump beam is switched off, and the shadowed beam switched on. In Fig. 18 we show two measured loading curves. One shows loading using the conventional method without the shadow and with reduced repump power, and the second curve shows the new method with the shadowed beam and increased repump power. The maximum number of loaded atoms doubles from 3.9×10^6 to 7.7×10^6. The transfer efficiency from MOT to FORT increased from 21% to 42%.

The increase in the number is caused by a decrease of the loss rate from $\beta_L' = (3.5 \pm 0.5) \times 10^{-6}$ s^{-1} to $\beta_L' = (1.7 \pm 0.3) \times 10^{-6}$ s^{-1} and a simultaneous increase of the loading rate, from $R_0 = 5.8 \times 10^7$ s^{-1} to $R_0 = 10.2 \times 10^7$ s^{-1}. The loading rate is increased, due to the fact that the MOT density increases, by reducing the repump intensity in the center of the MOT.

The loss rate β_L' is still larger during loading with the shadow than in the absence of all MOT light, where the loss rate $\beta' = 2.3 \times 10^{-7}$ s^{-1}. This is due to the fact that the MOT light is not shadowed and the FORT acts as a very weak repump laser. Thus, placing additional shadows in the main MOT light may improve the loading even more, but this requires a more complicated optical setup. By reducing β_L' to the limit of no MOT light, while maintaining the same loading rate, the steady state number of atoms will be 2 $\times 10^7$, nearly all of the MOT atoms.

X. CONCLUSIONS

Our study can be summarized as follows. Deeper traps load more atoms and the temperature is a fixed fraction of the trap depth. Optimum loading is achieved for very low repump scattering rate ($I_{RP} = 5$ μW/cm^2), and a MOT detuning that depends on the FORT depth. Controlling the geometry of the overlap of the MOT and FORT beams gives substantial improvement. To maximize the number of atoms trapped in the FORT, these are the parameters to adjust.

However, underneath this recipe lies a lot of interesting physics. Loading the FORT from a MOT is a dynamical process, governed by a loading rate R_0 and density dependent losses characterized by β_L'. During the loading, the MOT light fields increase the FORT loss rate considerably. The main loss mechanism during loading of the FORT is radiative escape collision induced by the MOT light fields. The loss rate is higher than in a MOT because the FORT is on the order of only a millikelvin deep, whereas a typical MOT is a kelvin deep. In addition, the light shift due to the FORT changes the hyperfine repump rate and the optical excitation by the MOT trapping and cooling light, which is responsible for the radiative escape. Taking these effects into account, we were able to model how the loss rate depends on the intensities and detunings of the primary MOT and repump lasers, as well as the FORT depth. This model explains the experimentally observed dependencies of the loss rate on these parameters quite well. The loading rate can be described in two parts: a flux of atoms into the volume of the FORT times a probability of being trapped. Both parts depend on the MOT and FORT parameters, including the size of the FORT.

Here we studied the loading of a FORT with a radius $\leqslant 60$ μm, which is much smaller than the radius of the MOT. Even with this mismatch of size between the MOT and the FORT, we were able to transfer more than 40% of the atoms initially trapped in the MOT to the FORT. For FORTs with a radius comparable to that of the MOT, the description of the loading rate changes, and the loss rate may also behave differently; however, we believe that radiative escape processes may still be enhanced as compared to a MOT. Working with a small waist enables one to make deeper traps and achieve tighter confinement. Such conditions may make it possible to reach, for instance, Bose-Einstein condensation at high temperatures of tens of microkelvins.

[1] S. Chu, J. E. Bjorkholm, A. Ashkin, and A. Cable, Phys. Rev. Lett. **57**, 314 (1986).

[2] E. L. Raab, M. Prentiss, A. Cable, S. Chu, and D. E. Pritchard, Phys. Rev. Lett. **59**, 2631 (1987); C. Monroe, W. Swann, H. Robinson, and C. Wieman, *ibid.* **65**, 1571 (1990).

[3] J. D. Miller, R. A. Cline, and D. J. Heinzen, Phys. Rev. A **47**, R4567 (1993).

[4] C. S. Adams, H. J. Lee, N. Davidson, M. Kasevich, and S. Chu, Phys. Rev. Lett. **74**, 3577 (1995).

[5] T. Takekoshi and R. J. Knize, Opt. Lett. **21**, 77 (1996).

[6] D. Boiron, A. Michaud, J. M. Fournier, L. Simard, M. Sprenger, G. Grynberg, and C. Salomon, Phys. Rev. A **57**, R4106 (1998).

[7] S. Bali, K. M. O'Hara, M. E. Gehm, S. R. Granade, and J. E. Thomas, Phys. Rev. A **60**, R29 (1999).

[8] H. C. W. Beijerinck, Phys. Rev. A **61**, 033606 (2000).

[9] M. E. Gehm, K. M. O'Hara, T. A. Savard, and J. E. Thomas, Phys. Rev. A **58**, 3914 (1998).

[10] T. Walker and P. Feng, Adv. At., Mol., Opt. Phys. **34**, 125 (1997).

[11] K. M. O'Hara, S. R. Granade, M. E. Gehm, T. A. Savard, S. Bali, C. Freed, and J. E. Thomas, Phys. Rev. Lett. **82**, 4204 (1999).

[12] A. E. Siegman, *Lasers* (University Science Books, Mill Valley, CA, 1986).

[13] D. Cho, J. Korean Phys. Soc. **30**, 373 (1997).

[14] C. Cohen-Tannoudji and J. Dupont-Roc, Phys. Rev. A **5**, 968 (1972).

[15] We define the ellipticity ϵ by writing the polarization vector of the light as $\hat{\epsilon} = 1/\sqrt{2}(\hat{x}\sqrt{1+\epsilon} + i\hat{y}\sqrt{1-\epsilon})$.

[16] K. L. Corwin, Zheng Tian Lu, C. F. Hand, R. J. Epstein, and C. E. Wieman, Appl. Opt. **37**, 3295 (1998).

[17] C. G. Townsend, N. H. Edwards, C. J. Cooper, K. P. Zetie, C. J. Foot, A. M. Steane, P. Szriftgiser, H. Perrin, and J. Dalibard, Phys. Rev. A **52**, 1423 (1995).

[18] K. L. Corwin, S. J. M. Kuppens, D. Cho, and C. E. Wieman, Phys. Rev. Lett. **83**, 1311 (1999).

[19] J. D. Miller, Ph.D. thesis, University of Texas, 1994.

[20] A. Gallagher and D. E. Pritchard, Phys. Rev. Lett. **63**, 957 (1989).

[21] P. D. Lett, K. Molmer, S. D. Gensemer, K.-Y. N. Tan, A. Kumarakrishnan, C. D. Wallace, and P. L. Gould, J. Phys. B **28**, 65 (1995).

[22] P. S. Julienne and J. Vigue, Phys. Rev. A **44**, 4464 (1991).

[23] S. D. Gensemer, V. Sanchez-Villicana, K.-Y. N. Tan, T. T. Grove, and P. L. Gould, Phys. Rev. A **56**, 4055 (1997).

[24] D. Sesko, T. Walker, C. Monroe, A. Gallagher, and C. Wieman, Phys. Rev. Lett. **63**, 961 (1989).

[25] C. D. Wallace, T. P. Dinneen, K.-Y. N. Tan, T. T. Grove, and P. L. Gould, Phys. Rev. Lett. **69**, 897 (1992).

[26] L. Marcassa, V. Bagnato, Y. Wang, C. Tsao, J. Weiner, O. Dulieu, Y. B. Band, and P. S. Julienne, Phys. Rev. A **47**, R4563 (1993).

[27] M. G. Peters, D. Hoffmann, J. D. Tabiason, and T. Walker, Phys. Rev. A **50**, R906 (1994).

[28] D. Hoffmann, P. Feng, and T. Walker, J. Opt. Soc. Am. B **11**, 712 (1994).

[29] M. Drewsen, Ph. Laurent, A. Nadir, G. Santarelli, A. Clairon, Y. Castin, D. Grison, and C. Salomon, Appl. Phys. B: Lasers Opt. **59**, 283 (1994).